How Cation Migration Across 2D/3D Interface Dictates Perovskite Solar Cell Efficiency

Gábor Szabó and Prashant V. Kamat*

Radiation Laboratory, Department of Chemistry and Biochemistry, and Department of Chemical and Biomolecular Engineering,

University of Notre Dame, Notre Dame, Indiana 46556, United States

*Address correspondence to this author pkamat@nd.edu

Abstract

Perovskite solar cells with 2D/3D architecture are claimed to exhibit better stability as compared to pristine 3D films at room temperature. However, under illumination and/or heat, cation migration causes the exchange of the bulky spacer cations (2D phase) with the smaller A-site cations (3D phase), creating a gradient heterostructure at the 2D/3D interface. We have evaluated the performance of $BA_2MAPb_2I_7/MAPbI_3$ (2D/3D) and $MAPbI_3$ (3D) solar cells at different temperatures, while simultaneously probing the absorption changes of the 2D/3D perovskite layer and photovoltaic performance of solar cell devices. The 2D/3D solar cells were more stable at room temperature, but exhibited deterioration of photovoltaic performance at high temperatures. By employing in-situ measurements of operating solar cells to track both the photoconversion efficiency and absorption changes at different temperatures, we show that the cation exchange at the 2D/3D interface contributes to the efficiency losses.

TOC Graphic

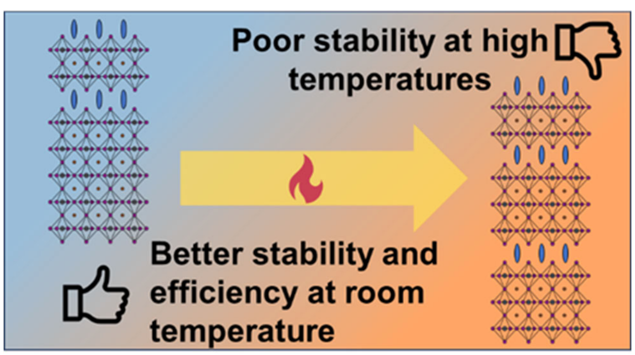

Perovskite solar cells (PSCs) have emerged as one of the exciting candidates in solar energy conversion devices. The progress made regarding the cell architecture to achieve power conversion efficiency compatible with Si photovoltaics has drawn the attention towards commercialization.[1, 2] However, in recent years, the increase in efficiency has only been incremental, mostly achieved by decreasing cell area.[2, 3] Increasing the cell area without significant losses and with improved stability remains a challenge.[2]

Significant efforts are being made to improve long-term stability in PSCs. The initial effort was to introduce alloying of A-site cations and halide ions in 3D perovskites.[4-10] Surface treatments have been widely employed to passivate surface defects and achieve long-term stability.[8, 10-21] Another approach involves depositing a 2D perovskite phase on top of the 3D perovskite phase thus creating a 2D/3D architecture for solar cell operation.[8, 10, 12-18, 21, 22] In a 2D/3D architecture of perovskite solar cells, the 3D perovskite phase is responsible for efficient photon conversion, while the 2D perovskite phase provides stability against moisture due to the hydrophobic spacer cations.[23-26] This architecture has been shown to improve the long-term stability of PSCs at room temperature, and in some cases, even to improve the photon conversion efficiency.[8, 10, 12-15, 18, 22, 25, 27, 28] However, studies from several groups, as well as ours, have recently shown the dynamic nature of the 2D/3D interface, as it becomes unstable under thermal stress or light soaking.[19, 21, 29-35] The 2D/3D interface undergoes a transformation because of slow cation exchange, thus replacing the sharp 2D/3D interface with a gradient structure of 2D phases (n = 1, 2, 3, …).[29-31, 36] The cation exchange rate depends on the cation (both A-site and spacer cations), with alkylammonium ions such as butylammonium showing greater mobility under thermal and light stress compared to other more bulky spacer cations.[29, 37-39] It has been shown that at elevated temperatures, for example at 50 °C, the deterioration of 2D/3D interface results in the efficiency loss of perovskite solar cells.[33] A recent report suggests that at higher temperatures (85 °C) the

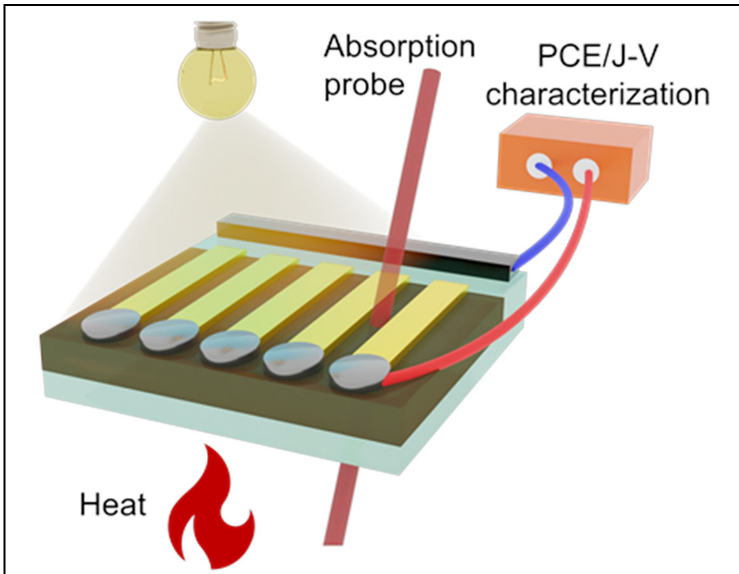

Scheme 1. 2D/3D solar cell architecture allowing absorption measurements between 2 metal contacts.

stability of the perovskite solar cells with 2D/3D architecture performs poorly compared to 3D PSC without the 2D layer.[32]

The unstable nature of the 2D/3D interface leads to the question of how the cation exchange affects the solar cell performance. In order to correlate the changes at the 2D/3D interface to solar cell performance, we have now conducted a systematic study of probing absorption changes and solar cell performance using a templated solar cell. The solar cell architecture employed in this study provides a sufficient gap between 2 metal contacts to carry out absorbance measurements of the active layer of the solar cell while subjecting it to thermal stress (Scheme 1). The results that correlate the solar cell characteristics with the absorption changes associated with 2D/3D interface are discussed.

3D and 2D/3D solar cells at room temperature

The solar cells in this study were fabricated with a thin 3D $MAPbI_3$ perovskite layer deposited on an electron transport layer (TiO_2). The layer thickness was carefully controlled to enable probing of absorption changes in the visible region. The concentration of the methylammonium lead halide precursor solution was lower than that of commonly employed precursor solutions. We also employed higher concentration of butylammonium iodide (BAI) to deposit a 2D film on top of the 3D perovskite layer. With a relatively thicker 2D layer on top of the 3D film, we were able to probe the absorption changes in the 2D layer (See SI for experimental details and the concentrations of precursor solutions). The hole conducting layer (Spiro-MeOTAD) was deposited on the top of 2D/3D perovskite layer, followed by the evaporation of gold for electrical contact. For performance comparison, solar cells without a 2D layer were also constructed using the same methodology. A fully operating cell created using this method allowed us to probe both absorption changes and solar cell performance during 1 sun (AM 1.5G, 100 mW/cm^2) photoirradiation after treating at different temperatures.

Figure 1A shows the absorption spectra of perovskite solar cell constructed with 3D and 2D/3D layers. Both these cells show an onset of absorption below 800 nm corresponding to the bandgap of the 3D phase ($MAPbI_3$). The solar cell consisting of 2D/3D phases shows an additional absorption peak at 570 nm, indicating the presence of the 2D layer. Although we deposited butylammonium iodide on top of $MAPbI_3$ film to create a 2D layer, the mixing of two cations (BA and MA) led to the formation of n=2 layer in the 2D phase ($BA_2MAPb_2I_7$), as confirmed from the absorption peak position at 570 nm. [29, 35, 40]

The photocurrent response of both cells recorded in terms of IPCE is presented in Figure 1B. The onset current observed below 800 nm matches the absorption onset observed for both cells. Both these cells exhibit similar profiles for photocurrent response, indicating minimal contribution of the 2D layer in the overall photocurrent generation. However, the J-V (current density-voltage) curves (Figure 1C) show lower power conversion efficiency (PCE) for the 2D/3D based cells. As indicated above, a slightly thicker 2D layer deposited in the present case (to probe 2D phase through absorbance measurements) is likely to be responsible for the decreased efficiency. Nevertheless, we can compare the performance of these cells to test their stability. The normalized PCE for the two cells recorded in Figure 1C (average of 18 individual measurements) shows the stability of the two cells over the period of 168 hours (1 week). The cells were stored in a glovebox (N_2 atmosphere) and periodically removed to evaluate the photovoltaic performance under ambient conditions. After completing each measurement, we returned the solar cells to the glovebox for storage. This allowed us to exclude any moisture effects that one may encounter during storage under ambient conditions.

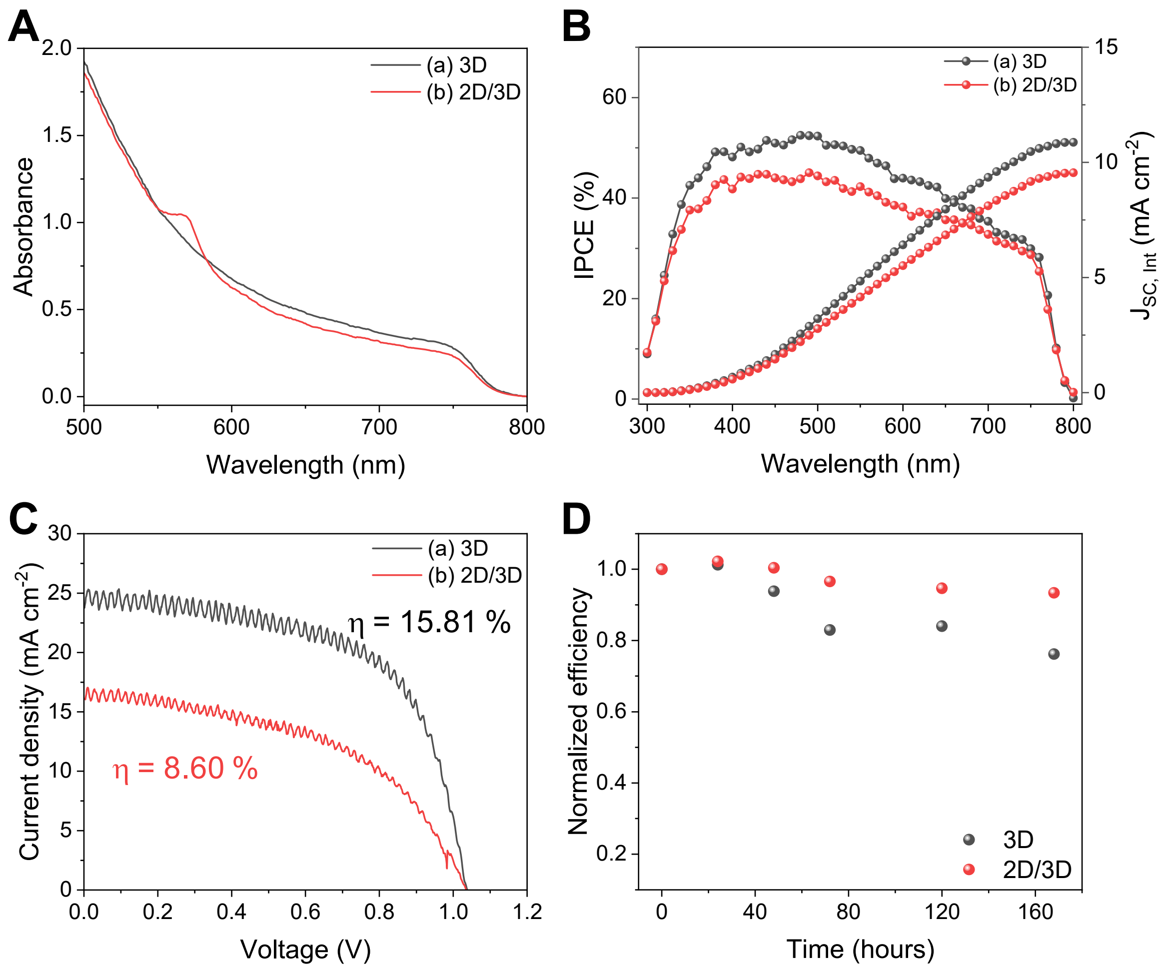

Figure 1. Characterization of 3D and 2D/3D perovskite solar cells at room temperature. (A) Absorption spectra of fresh 3D and 2D/3D perovskite films in solar cells. (B) Representative IPCE spectra and integrated short circuit current densities of fresh 3D and 2D/3D perovskite solar cells. (C) Representative J-V curves of fresh 3D and 2D/3D perovskite solar cells. The curves were obtained by scanning from 1.2 V to -0.1 V (reverse scan) at 50 mV/s scan rate during 1 sun (AM 1.5G, 100 mW/cm^2) illumination. (D) Normalized efficiency of 3D and 2D/3D solar cells in one week at room temperature, calculated from J-V curves. Cell area was 0.11 cm^2. Solar cells were kept in a N_2-filled glovebox between measurements.

Overall, 2D/3D solar cells exhibited better stability than 3D solar cells, which is consistent with the earlier reports.[12, 15, 18, 27] The 2D/3D perovskite solar cells lost ~10% of their initial efficiency during storage in a period of one week. We observed a small decrease in the 2D absorbance at 570 nm during the same period of storage, thus indicating loss of the 2D phase as a result of cation exchange.[29, 30] The absorption spectra showed negligible changes for the 3D solar cells, yet the relative decrease in PCE was more than that of 2D/3D PSCs. (The absorption spectra of the perovskite films over time are presented in Figure S1 and S2.) These results suggest that the deposition of 2D layer makes the solar cell more stable compared to 3D PSC under N_2 storage, but still exhibits some degree of instability. As pointed out earlier, cation (BA and MA) migration between the 2D and 3D phases is likely to disrupt the interface of the two phases, causing the PSC performance to decrease.

Stability at higher storage temperature

In order to assess the stability of PSCs at higher temperatures, we evaluated solar cell performance at 60 °C. If PSC panels must be installed outdoors, one needs to take into consideration higher operating temperatures (usually 60-80 °C).[41, 42] Thus, it becomes logical to further to test the stability of these solar cells at higher temperatures.

We evaluated the performance of the 3D and 2D/3D perovskite solar cells stored at 60 °C in N_2 atmosphere and carried out PSC performance evaluation at room temperature in air. Before removing the solar cells from the glovebox, they were allowed to cool down to room temperature. Figure 2 shows the J-V curves of both types of solar cells before and after being kept at 60 °C for 96 hours in a N_2-filled glovebox. Within this period, the 2D/3D solar cell lost ~50 % of its initial power conversion efficiency, while the 3D perovskite solar cell lost ~35 % of its starting value. The J-V curves show that both solar cells showed a decreased open-circuit voltage (V_{OC}) and fill factor

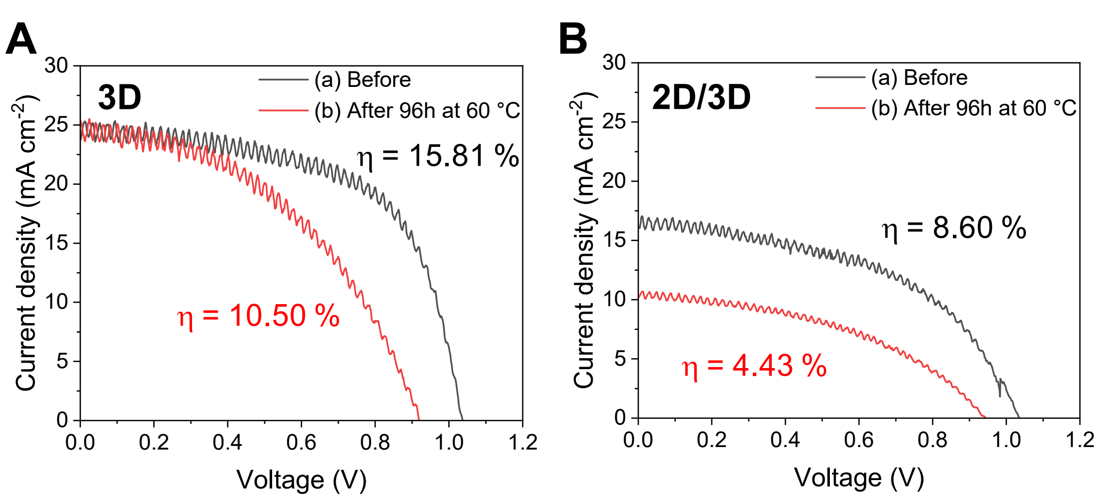

Figure 2. J-V curves of solar cells before and after annealing at 60 °C for 96 hours. (A) J-V curves of 3D solar cells before and after annealing. (B) J-V curves of 2D/3D solar cells before and after being kept at 96 °C. All J-V curves were obtained by scanning from 1.2 V to -0.1 V (reverse scan) at 50 mV/s scan rate during 1 sun (AM 1.5G, 100 mW/cm^2) illumination. The cell area was 0.11 cm^2 in all cases.

(FF) after being kept at 60 °C. However, only the 2D/3D solar cell had a significant decrease in the short-circuit current density (J_{SC}). We attribute this difference to the disruption of the 2D/3D interface resulting from the interaction between the 2D and 3D layers in a 2D/3D perovskite solar cell.

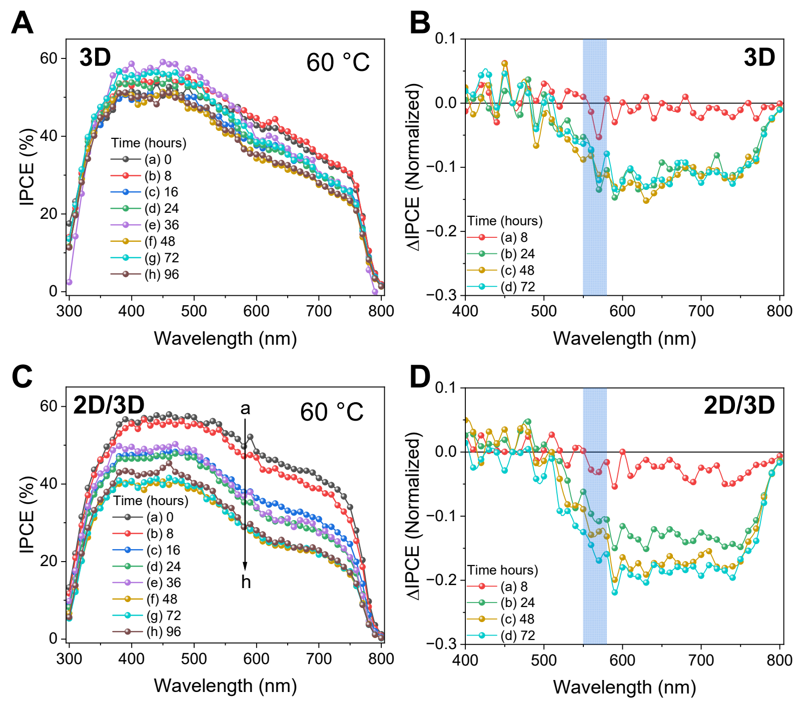

Figure 3. Evolution of IPCE spectra of PSCs kept at 60 °C. (A) IPCE spectra of 3D solar cell over time while kept at 60 °C. (B) Difference IPCE spectra obtained from spectra b-h in panel A, with spectrum a as reference. The blue rectangle highlights the region of the absorbance peak (570 nm) corresponding to the n=2 2D phase (C) IPCE spectra of 2D/3D solar cell recorded over time while kept at 60 °C. (D) Difference IPCE spectra obtained from spectra b-h in panel C, with spectrum a as reference. The blue rectangle highlights the region of the absorption peak (570 nm) related to $BA_2MAPb_2I_7$ (n=2)

To gain additional support for the argument that the observed change in the J_{SC} of the 2D/3D solar cell is indeed related to the interaction between the 2D and 3D layers, we took a closer look at the IPCE spectra of PSCs kept at 60 °C in a N_2-filled glovebox. Over 96 hours the 2D/3D perovskite solar cell showed a gradual decrease in the IPCE (Figure 3A). On the other hand, we observed only a small change in the IPCE of the 3D perovskite solar cell while stored at 60 °C for 96 hours (Figure 3C). This decrease in IPCE is consistent with the observations made from the analysis of the J-V curves.

To better visualize the changes in the IPCE spectra, we plotted the difference IPCE spectra following normalization. We normalized the IPCE spectra to the maximum value at 470 nm before determining the ΔIPCE. The decrease in IPCE at this wavelength was also small compared to the IPCE change in the longer wavelength region (Figures 3B and 3D). The change in the IPCE reflects the loss of absorption resulting from the instability of perovskite layers. The decrease in IPCE is greater for the 2D/3D PSC than that of the 3D PSC. This difference is especially noticeable in the 570 nm region (marked blue), at which the 2D phase (n=2) of perovskite dominates. As highlighted by the blue marked region in Figure 3B and 3D, we observed a small feature around 570 nm for the 2D/3D solar cell, but not for the 3D solar cell. The decrease in IPCE observed for 2D/3D PSCs corresponding to the absorbance peak of the n=2 $BA_2MAPb_2I_7$, further affirms our argument that the interaction of the 2D and 3D phases directly affects the performance of the solar cell.

Cation migration probed through absorption changes at different temperatures.

While evaluating the perovskite solar cell performance, we simultaneously carried out absorbance measurements. This procedure allowed us to probe the absorption changes associated with the decreased solar cell performance under the same set of conditions. The changes in the absorption spectra of 2D/3D solar cells kept at 60 °C in a N_2-filled glovebox are shown in Figures 4A and 4B. With increasing storage time, we see a decrease in the absorption of the perovskite layers. The decrease is more prominent in the 570 nm region in which 2D layer dominates the absorption. It

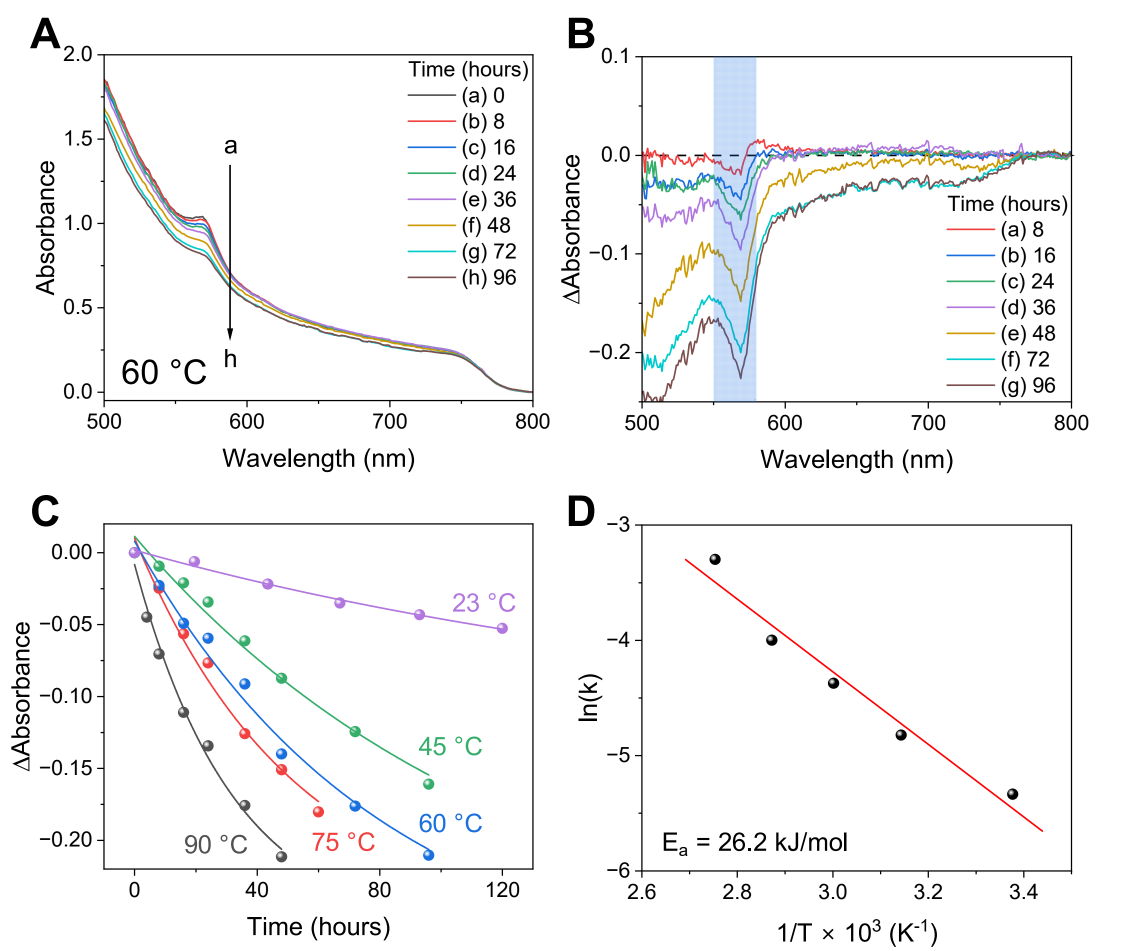

Figure 4. (A) Absorption spectra of a 2D/3D perovskite film in a device recorded over time while kept at 60 °C in a N_2-filled glovebox. (B) Difference absorption spectra obtained from spectra b-h in panel A, with spectrum a as reference. The blue rectangle highlights the absorption peak (570 nm) related to $BA_2MAPb_2I_7$ (n=2) (C) Changes in absorbance of the n=2 peak at 570 nm at different temperatures. (D) Arrhenius plot of the rate constants obtained from the fitted curves in panel C.

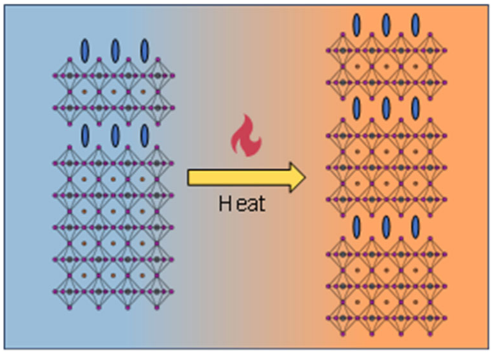

Scheme 2. Visualization of cation exchange between 2D and 3D phases.

is interesting to note that these absorbance changes are similar to the changes observed in IPCE (Figure 3B). The difference absorption spectra (Figure 4B) revealed that the absorbance corresponding to the 3D phase decreases as well, albeit to a much smaller extent. This suggests that both 2D and 3D phases are involved in exchanging cations, viz., BA and MA. The interaction between the 2D and 3D phases thus results in a gradient 2D phase involving multiple 2D phases (n=2, 3, 4, …), as depicted in Scheme 2. In a recent study we observed a similar exchange between BA and MA when 2D and 3D films cast on glass slides were physically paired and subjected to thermal stress. [29]

Since the decrease in the 570 nm absorbance represents a change in layer number of 2D phase from n=2 to higher number as BA cations migrate to 3D phase replaced by MA cations from 3D phase, we can follow the kinetics of cation migration between the two layers. Figure 4C shows the absorbance decay at 570 nm recorded at different temperatures. We fitted the absorbance decay to pseudo-first order kinetics. The rate constant of cation migration increased with increased temperature. By using the Arrhenius relationship, we determined the activation energy to be 26.2 kJ/mol (Figure 4D).

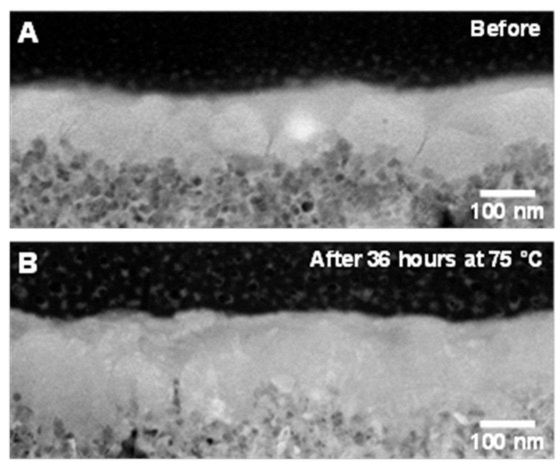

Figure 5. Cross-sectional high-angle annular dark-field (HAADF) image of the 2D/3D perovskite layer (A) of a fresh sample and (B) a sample after 36 hours of annealing at 75 °C.

To visualize the changes induced by the cation migration, we obtained cross-sectional high-angle annular dark-field (HAADF) images of fresh, and heat-treated (36 hours at 75 °C in N_2-filled glovebox) 2D/3D solar cells. Figure 5A shows the cross-section of a freshly prepared 2D/3D perovskite solar cell. The grey area in the middle corresponds to the 2D/3D perovskite layer. The large, brighter grains correspond to $MAPbI_3$, while the slightly darker regions above and in between the grains correspond to the 2D layer. The black layer above the perovskite is the spiro-MeOTAD hole transport layer, while the bottom layer is the mesoporous TiO_2 layer for electron transport. When the solar cell was kept at

75 °C for 36 hours, most changes occur at 2D/3D interface as cations are exchanged between the two layers. It is rather difficult to distinguish the 2D and 3D phases in Figure 5B, as the separation between the two phases has disappeared. As the phases with higher n values carry morphology and composition similar to the 3D phase than the 2D phase, the lack of contrast after heat treatment disappears. These results further support the claim of cation exchange disrupting the 2D/3D interface.

If the changes in absorption (Figure 4) observed because of the cation exchange at the 2D/3D interface, we should be able to track this phenomenon through the changes in PCE with time at different temperatures. We measured the power conversion efficiencies of 2D/3D and 3D perovskite solar cells which were employed for absorbance measurements in Figure 4. Figures 6A and 6B show the decay of the average normalized solar cell efficiencies of 2D/3D and 3D solar

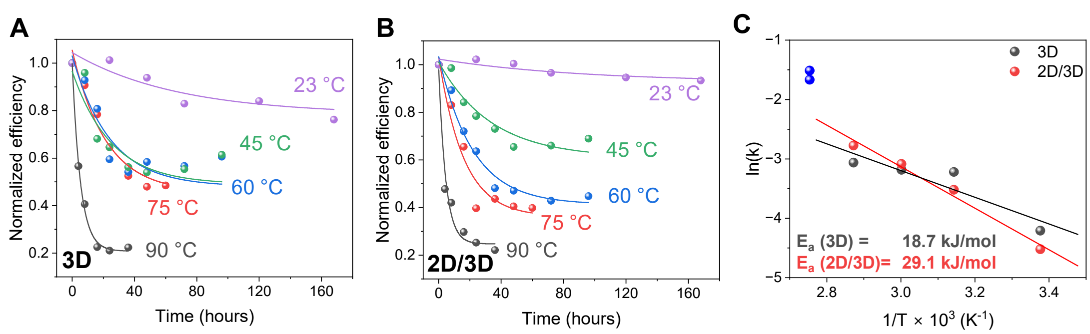

Figure 6. Normalized power conversion efficiency recorded over storage time at different temperatures (A) 3D solar cells and (B) 2D/3D solar cells. The PCE values were normalized at maximum value in each case. The data is an average of 18 solar cells. (C) Arrhenius plot of the rate constants for 3D and 2D/3D solar cells obtained from the fitted curves in panel A and B.

cells over the period of storage time at different temperatures. The distributions of solar cell efficiencies are shown in the supporting information in Figures S3-6. Similar to the changes in absorbance, we fitted pseudo-first order kinetics to the decay of the normalized efficiency for both 3D and 2D/3D solar cells. At lower temperature (23°C) the decay of IPCE of 3D solar cell was faster than that of 2D/3D solar cell. However, a reverse trend (viz., greater rate constant at higher temperatures was noted for 2D/3D solar cell. Figure 6C shows the dependence of logarithmic rate constant of decreased PCE versus inverse of temperature. The activation energy obtained from the Arrhenius plot in Figure 6C was 29.3 kJ/mol for the 2D/3D solar cell. This value agrees with the activation energy (26.2 kJ/mol) determined from the absorption measurements in Figure 4D. Interestingly, solar cells with only 3D perovskite film show lesser dependence on the temperature and lower activation energy (18.7 kJ/mol). These results provide additional evidence that cation migration between the 2D/3D layers is responsible for the efficiency loss of 2D/3D perovskite solar cells. The efficiency drop is greater at higher temperature for these cells.

By now it has become a common practice in perovskite solar cell fabrication to use a protective 2D layer to enhance stability and efficiency. However, it has been established that such interfaces are not stable, because 2D and 3D phases interact via cation exchange, forming new phases in-between. By comparing absorbance and IPCE measurements we were able to conclude cation migration between 2D/3D layers as a major contributor to the decreasing performance. The good match between the activation energies obtained from the absorption spectra and efficiency decays proves that the cation exchange dictates the performance of 2D/3D solar cells. Even though 2D/3D solar cells are more stable than 3D solar cells at room temperature, the cation exchange still progresses slowly and affects the solar cell performance over long term storage. However, increased cation migration rate at elevated temperatures, cause 2D/3D solar cells to perform worse than the 3D solar cells. Careful selection of other spacer cations and alloying with other A-site cations (like FA^+, Cs^+) may extend the time of stable performance of the 2D/3D perovskite solar cell. However, the delay in photovoltaic performance is inevitable if one has to account ion migration as an intrinsic property of lead halide perovskites.

Acknowledgment

The work is supported by the Division of Materials Sciences and Engineering Office of Basic Energy Sciences of the U.S. Department of Energy through Award DE-SC0014334 to study the ion migration effects in metal halide perovskites. P.V.K. acknowledges support by the Division of Chemical Sciences, Geosciences, and Biosciences, Office of Basic Energy Sciences of the U.S. Department of Energy (award DE-FC02- 04ER15533). This is contribution number No. 5417 from the Notre Dame Radiation Laboratory.

Supporting information

Experimental details (materials, solar cell preparation, characterization), additional absorption spectra, and distribution of solar cell efficiencies.

References

(1) Yoo, J. J.; Shin, S. S.; Seo, J. Toward Efficient Perovskite Solar Cells: Progress, Strategies, and Perspectives. *ACS Energy Letters* **2022**, *7* (6), 2084-2091.

(2) Zhu, H.; Teale, S.; Lintangpradipto, M. N.; Mahesh, S.; Chen, B.; Mcgehee, M. D.; Sargent, E. H.; Bakr, O. M. Long-Term Operating Stability in Perovskite Photovoltaics. *Nature Reviews Materials* **2023**, *8* (9), 569-586.

(3) *NREL, PIP & NREL Data Cell Efficiency Table*. https://www.nrel.gov/pv/assets/docs/cell-efficiency-data-table.xlsx (accessed 2023-10-27).

(4) Saliba, M.; Matsui, T.; Seo, J.-Y.; Domanski, K.; Correa-Baena, J.-P.; Nazeeruddin, M. K.; Zakeeruddin, S. M.; Tress, W.; Abate, A.; Hagfeldt, A.; et al. Cesium-Containing Triple Cation Perovskite Solar Cells: Improved Stability, Reproducibility and High Efficiency. *Energy & Environmental Science* **2016**, *9* (6), 1989-1997.

(5) Pellet, N.; Gao, P.; Gregori, G.; Yang, T. Y.; Nazeeruddin, M. K.; Maier, J.; Grätzel, M. Mixed-Organic-Cation Perovskite Photovoltaics for Enhanced Solar-Light Harvesting. *Angewandte Chemie International Edition* **2014**, *53* (12), 3151-3157.

(6) Mundt, L. E.; Zhang, F.; Palmstrom, A. F.; Xu, J.; Tirawat, R.; Kelly, L. L.; Stone, K. H.; Zhu, K.; Berry, J. J.; Toney, M. F.; et al. Mixing Matters: Nanoscale Heterogeneity and Stability in Metal Halide Perovskite Solar Cells. *ACS Energy Letters* **2022**, *7* (1), 471-480.

(7) Xu, J.; Boyd, C. C.; Yu, Z. J.; Palmstrom, A. F.; Witter, D. J.; Larson, B. W.; France, R. M.; Werner, J.; Harvey, S. P.; Wolf, E. J.; et al. Triple-Halide Wide–Band Gap Perovskites with Suppressed Phase Segregation for Efficient Tandems. *Science* **2020**, *367* (6482), 1097-1104.

(8) Wang, Z.; Lin, Q.; Chmiel, F. P.; Sakai, N.; Herz, L. M.; Snaith, H. J. Efficient Ambient-Air-Stable Solar Cells with 2D–3D Heterostructured Butylammonium-Caesium-Formamidinium Lead Halide Perovskites. *Nature Energy* **2017**, *2* (9), 17135.

(9) An, Y.; Hidalgo, J.; Perini, C. A. R.; Castro-Méndez, A.-F.; Vagott, J. N.; Bairley, K.; Wang, S.; Li, X.; Correa-Baena, J.-P. Structural Stability of Formamidinium- and Cesium-Based Halide Perovskites. *ACS Energy Letters* **2021**, *6* (5), 1942-1969.

(10) Proppe, A. H.; Johnston, A.; Teale, S.; Mahata, A.; Quintero-Bermudez, R.; Jung, E. H.; Grater, L.; Cui, T.; Filleter, T.; Kim, C.-Y.; et al. Multication Perovskite 2D/3D Interfaces Form Via Progressive Dimensional Reduction. *Nature Communications* **2021**, *12* (1), 3472.

(11) Wang, F.; Shimazaki, A.; Yang, F.; Kanahashi, K.; Matsuki, K.; Miyauchi, Y.; Takenobu, T.; Wakamiya, A.; Murata, Y.; Matsuda, K. Highly Efficient and Stable Perovskite Solar Cells by Interfacial Engineering Using Solution-Processed Polymer Layer. *The Journal of Physical Chemistry C* **2017**, *121* (3), 1562-1568.

(12) Grancini, G.; Roldán-Carmona, C.; Zimmermann, I.; Mosconi, E.; Lee, X.; Martineau, D.; Narbey, S.; Oswald, F.; De Angelis, F.; Graetzel, M.; et al. One-Year Stable Perovskite Solar Cells by 2D/3D Interface Engineering. *Nature Communications* **2017**, *8* (1), 15684.

(13) Cho, K. T.; Grancini, G.; Lee, Y.; Oveisi, E.; Ryu, J.; Almora, O.; Tschumi, M.; Schouwink, P. A.; Seo, G.; Heo, S.; et al. Selective Growth of Layered Perovskites for Stable and Efficient Photovoltaics. *Energy & Environmental Science* **2018**, *11* (4), 952-959.

(14) Lee, J.-W.; Dai, Z.; Han, T.-H.; Choi, C.; Chang, S.-Y.; Lee, S.-J.; De Marco, N.; Zhao, H.; Sun, P.; Huang, Y.; et al. 2D Perovskite Stabilized Phase-Pure Formamidinium Perovskite Solar Cells. *Nature Communications* **2018**, *9* (1), 3021.

(15) Jang, Y.-W.; Lee, S.; Yeom, K. M.; Jeong, K.; Choi, K.; Choi, M.; Noh, J. H. Intact 2D/3D Halide Junction Perovskite Solar Cells Via Solid-Phase in-Plane Growth. *Nature Energy* **2021**, *6* (1), 63-71.

(16) Lin, Y.; Bai, Y.; Fang, Y.; Chen, Z.; Yang, S.; Zheng, X.; Tang, S.; Liu, Y.; Zhao, J.; Huang, J. Enhanced Thermal Stability in Perovskite Solar Cells by Assembling 2D/3D Stacking Structures. *The Journal of Physical Chemistry Letters* **2018**, *9* (3), 654-658.
(17) La-Placa, M.-G.; Gil-Escrig, L.; Guo, D.; Palazon, F.; Savenije, T. J.; Sessolo, M.; Bolink, H. J. Vacuum-Deposited 2D/3D Perovskite Heterojunctions. *ACS Energy Letters* **2019**, *4* (12), 2893-2901.
(18) Sidhik, S.; Wang, Y.; De Siena, M.; Asadpour, R.; Torma, A. J.; Terlier, T.; Ho, K.; Li, W.; Puthirath, A. B.; Shuai, X.; et al. Deterministic Fabrication of 3D/2D Perovskite Bilayer Stacks for Durable and Efficient Solar Cells. *Science* **2022**, *377* (6613), 1425-1430.
(19) Fiorentino, F.; Albaqami, M. D.; Poli, I.; Petrozza, A. Thermal- and Light-Induced Evolution of the 2D/3D Interface in Lead-Halide Perovskite Films. *ACS Applied Materials & Interfaces* **2022**, *14* (30), 34180-34188.
(20) Niu, T.; Lu, J.; Munir, R.; Li, J.; Barrit, D.; Zhang, X.; Hu, H.; Yang, Z.; Amassian, A.; Zhao, K.; et al. Stable High-Performance Perovskite Solar Cells Via Grain Boundary Passivation. *Advanced Materials* **2018**, *30* (16), 1706576.
(21) Luo, L.; Zeng, H.; Wang, Z.; Li, M.; You, S.; Chen, B.; Maxwell, A.; An, Q.; Cui, L.; Luo, D.; et al. Stabilization of 3D/2D Perovskite Heterostructures Via Inhibition of Ion Diffusion by Cross-Linked Polymers for Solar Cells with Improved Performance. *Nature Energy* **2023**, *8* (3), 294-303.
(22) Kim, S.-G.; De Monfreid, T.; Kim, J.-H.; Goubard, F.; Berry, J. J.; Zhu, K.; Bui, T.-T.; Park, N.-G. Nanographene Coupled with Interfacial Pyrene Derivatives for Thermally Stable Perovskite Solar Cells. *ACS Energy Letters* **2023**, *8* (5), 2267-2275.
(23) Grancini, G.; Nazeeruddin, M. K. Dimensional Tailoring of Hybrid Perovskites for Photovoltaics. *Nature Reviews Materials* **2018**, *4* (1), 4-22.
(24) Quan, L. N.; Yuan, M.; Comin, R.; Voznyy, O.; Beauregard, E. M.; Hoogland, S.; Buin, A.; Kirmani, A. R.; Zhao, K.; Amassian, A.; et al. Ligand-Stabilized Reduced-Dimensionality Perovskites. *Journal of the American Chemical Society* **2016**, *138* (8), 2649-2655.
(25) Bouduban, M. E. F.; Queloz, V. I. E.; Caselli, V. M.; Cho, K. T.; Kirmani, A. R.; Paek, S.; Roldan-Carmona, C.; Richter, L. J.; Moser, J. E.; Savenije, T. J.; et al. Crystal Orientation Drives the Interface Physics at Two/Three-Dimensional Hybrid Perovskites. *The Journal of Physical Chemistry Letters* **2019**, *10* (19), 5713-5720.
(26) Tsai, H.; Nie, W.; Blancon, J.-C.; Stoumpos, C. C.; Asadpour, R.; Harutyunyan, B.; Neukirch, A. J.; Verduzco, R.; Crochet, J. J.; Tretiak, S.; et al. High-Efficiency Two-Dimensional Ruddlesden–Popper Perovskite Solar Cells. *Nature* **2016**, *536* (7616), 312-316.
(27) Cho, Y.; Soufiani, A. M.; Yun, J. S.; Kim, J.; Lee, D. S.; Seidel, J.; Deng, X.; Green, M. A.; Huang, S.; Ho-Baillie, A. W. Y. Mixed 3D–2D Passivation Treatment for Mixed-Cation Lead Mixed-Halide Perovskite Solar Cells for Higher Efficiency and Better Stability. *Advanced Energy Materials* **2018**, *8* (20), 1703392.
(28) Lee, D. S.; Yun, J. S.; Kim, J.; Soufiani, A. M.; Chen, S.; Cho, Y.; Deng, X.; Seidel, J.; Lim, S.; Huang, S.; et al. Passivation of Grain Boundaries by Phenethylammonium in Formamidinium-Methylammonium Lead Halide Perovskite Solar Cells. *ACS Energy Letters* **2018**, *3* (3), 647-654.
(29) Mathew, P. S.; Kamat, P. V. Cation Migration in Physically Paired 2D and 3D Lead Halide Perovskite Films. *Advanced Optical Materials* **2023**, 2300957.
(30) Chakkamalayath, J.; Hiott, N.; Kamat, P. V. How Stable Is the 2D/3D Interface of Metal Halide Perovskite under Light and Heat? *ACS Energy Letters* **2023**, *8* (1), 169-171.
(31) Perini, C. A. R.; Rojas-Gatjens, E.; Ravello, M.; Castro-Mendez, A. F.; Hidalgo, J.; An, Y.; Kim, S.; Lai, B.; Li, R.; Silva-Acuña, C.; et al. Interface Reconstruction from Ruddlesden–Popper Structures Impacts Stability in Lead Halide Perovskite Solar Cells. *Advanced Materials* **2022**, *34* (51), 2204726.
(32) Wang, M.; Shi, Z.; Fei, C.; Deng, Z. J. D.; Yang, G.; Dunfield, S. P.; Fenning, D. P.; Huang, J. Ammonium Cations with High pKa in Perovskite Solar Cells for Improved High-Temperature Photostability. *Nature Energy* **2023**, *8*, 1229-1239.

(33) Sutanto, A. A.; Szostak, R.; Drigo, N.; Queloz, V. I. E.; Marchezi, P. E.; Germino, J. C.; Tolentino, H. C. N.; Nazeeruddin, M. K.; Nogueira, A. F.; Grancini, G. In Situ Analysis Reveals the Role of 2D Perovskite in Preventing Thermal-Induced Degradation in 2D/3D Perovskite Interfaces. *Nano Letters* **2020**, *20* (5), 3992-3998.
(34) Kodalle, T.; Moral, R. F.; Scalon, L.; Szostak, R.; Abdelsamie, M.; Marchezi, P. E.; Nogueira, A. F.; Sutter-Fella, C. M. Revealing the Transient Formation Dynamics and Optoelectronic Properties of 2D Ruddlesden-Popper Phases on 3D Perovskites. *Advanced Energy Materials* **2023**, *13* (33), 2201490.
(35) Stoumpos, C. C.; Cao, D. H.; Clark, D. J.; Young, J.; Rondinelli, J. M.; Jang, J. I.; Hupp, J. T.; Kanatzidis, M. G. Ruddlesden–Popper Hybrid Lead Iodide Perovskite 2D Homologous Semiconductors. *Chemistry of Materials* **2016**, *28* (8), 2852-2867.
(36) Sutanto, A. A.; Drigo, N.; Queloz, V. I. E.; Garcia-Benito, I.; Kirmani, A. R.; Richter, L. J.; Schouwink, P. A.; Cho, K. T.; Paek, S.; Nazeeruddin, M. K.; et al. Dynamical Evolution of the 2D/3D Interface: A Hidden Driver Behind Perovskite Solar Cell Instability. *Journal of Materials Chemistry A* **2020**, *8* (5), 2343-2348.
(37) Roy, C. R.; Pan, D.; Wang, Y.; Hautzinger, M. P.; Zhao, Y.; Wright, J. C.; Zhu, Z.; Jin, S. Anion Exchange of Ruddlesden–Popper Lead Halide Perovskites Produces Stable Lateral Heterostructures. *Journal of the American Chemical Society* **2021**, *143* (13), 5212-5221.
(38) Mathew, P. S.; Dubose, J. T.; Cho, J.; Kamat, P. V. Spacer Cations Dictate Photoinduced Phase Segregation in 2D Mixed Halide Perovskites. *ACS Energy Letters* **2021**, *6* (7), 2499-2501.
(39) Mathew, P. S.; Szabó, G.; Kuno, M.; Kamat, P. V. Phase Segregation and Sequential Expulsion of Iodide and Bromide in Photoirradiated Ruddlesden–Popper 2D Perovskite Films. *ACS Energy Letters* **2022**, *7* (11), 3982-3988.
(40) Cao, D. H.; Stoumpos, C. C.; Farha, O. K.; Hupp, J. T.; Kanatzidis, M. G. 2D Homologous Perovskites as Light-Absorbing Materials for Solar Cell Applications. *Journal of the American Chemical Society* **2015**, *137* (24), 7843-7850.
(41) Choi, K.; Lee, J.; Choi, H.; Kim, G.-W.; Kim, H. I.; Park, T. Heat Dissipation Effects on the Stability of Planar Perovskite Solar Cells. *Energy & Environmental Science* **2020**, *13* (12), 5059-5067.
(42) Pescetelli, S.; Agresti, A.; Viskadouros, G.; Razza, S.; Rogdakis, K.; Kalogerakis, I.; Spiliarotis, E.; Leonardi, E.; Mariani, P.; Sorbello, L.; et al. Integration of Two-Dimensional Materials-Based Perovskite Solar Panels into a Stand-Alone Solar Farm. *Nature Energy* **2022**, *7* (7), 597-607.